www.elsevier.com/locate/ijadhadh

SilanQe QSSurface Modification Of Boron Carbide In Epoxy Composites

D.D. Rodrigues, J.G. Broughton

PII: S0143-7496(13)00101-2
DOI: http://dx.doi.org/10.1016/j.ijadhadh.2013.05.014
Reference: JAAD1370

To appear in: *International Journal of Adhesion & Adhesives*

Received date: 1 September 2012
Accepted date: 7 May 2013

Cite this article as: D.D. Rodrigues, J.G. Broughton, SilanQe QSSurface Modification Of Boron Carbide In Epoxy Composites, *International Journal of Adhesion & Adhesives,* http://dx.doi.org/10.1016/j.ijadhadh.2013.05.014

SILANE SURFACE MODIFICATION OF BORON CARBIDE IN EPOXY COMPOSITES

D. D. Rodrigues*, J. G. Broughton

Joining Technology Research Centre, Oxford Brookes University (OBU), Wheatley Campus, OX33 1HX, UK

*Corresponding author. Tel.: +44 (0) 1865 482723; fax: +44 (0) 1865+44 (0) 1865 484 179. E-mail: david.rodrigues@brookes.ac.uk (D. D. Rodrigues).

Abstract

Boron carbide (BC) is a boron-rich ceramic material used as a radiation absorber for shielding parts in the nuclear industry and for particle physics experimentation. BC parts are generally manufactured using the sintering process, which tends to limit the size and shape of components and imparts high cost. Low temperature and lower pressure moulding using a BC polymer matrix composites (PMC) provides an alternative process for developing lower cost parts whilst accommodating increased complexity of geometry and size. However, a lack of adhesion exhibited between BC and the resin led to a composite with limited mechanical strength and durability. In this study a silane coupling agent was used to improve the adhesion between the epoxy resin and BC. An improvement in mechanical strength was observed in the treated composite by means of three-point bending, Iosipescu and double v-notch tests. Initial investigation of the surface chemistry also showed the presence of hydroxyl groups and B-O bonds, which may promote improved adhesion through silane condensation and the formation of covalent bonds.

Keywords: Boron carbide; epoxy; silane treatment; surface analysis; mechanical properties.

1. Introduction

Boron carbide (BC) is a non-oxide ceramic material used as a neutron absorber and shielding material, both to protect humans and sensitive instruments from stray neutron radiation. BC is typically employed in highly sensitive instruments where size is limited (e.g. space applications), due to its specific neutron high absorption/low scattering and relatively low production cost. BC parts can be produced using the solid state sinter process, although it is one of the more difficult materials to sinter due to its covalent nature, low mobility, high melting point, high hardness and brittle character [1]. On the other hand, a high BC content epoxy polymeric matrix composite (BE-PMC) can be easily made through a moulding process to obtain lower cost parts with increased complexity of geometry and size [2-4]. Epoxy resins themselves exhibit an excellent combination of properties and good durability to aggressive environments, including exposure to gamma rays and neutron radiation [5,6]. The function of the epoxy is to bond the particles together and transmit load. Therefore, these composites are built up from a complex interplay of physical and chemical factors that occur in the interface or interphase regions between the two materials and will determine the macroscopic properties and durability of the composite [7]. However, their long-term properties are not easy to predict, being only used in a limited number of well-proven applications. Very few studies have been published using BC in an epoxy resin matrix [2-4]. Of these, low BC content provided the best performance, as a result of a more uniform dispersion of filler, whereas, agglomeration and deposition in the resin was observed with higher BC contents. Moreover, the poor adhesion between the BC and epoxy led to BE-PMC with limited mechanical strength and durability.

Silane coupling agents have been widely employed to enhance the adhesion between polymer and inorganic materials, and to increase durability, by modifying the particle surface and the

bonding process at the interface. The result is the formation of a chemical bridge between the materials, higher hydrophobicity to prevent moisture penetration, better transfer of stress from the resin to the filler, more efficient dispersion of the filler and reduction of the apparent viscosity of the uncured system. The silane treatment is generally applied as an aqueous solution on the material surface and is highly dependent on a number of preparation/application parameters [7-10]. Despite the extensive use of silanes as adhesion promoters most, if not all, current applications are based on empirical formulations and procedures. Therefore, the most efficient preparation and application methods, as well as the mechanisms by which these agents enhance the bond strength and durability, are not fully understood. No such cases involving BC have been reported in the open literature, although related research seems to indicate that silanes could improve the adhesion between the BC and epoxy matrix. For example, a study was conducted to investigate the surface chemistry of boron fibres with plasma and/or silane treatment [11]. The mechanical tests confirmed an increase in adhesion between the materials, especially when a plasma process was applied prior to the silane treatment. The work suggested the plasma treatment increased the boron-oxygen containing species on the surface, providing increased attachment sites for the silane. In addition, B-O-Si fragments were found using time-of-flight secondary ion mass spectrometry (TOF-SIMS), despite the lack of evidence of a mechanism of attachment. Boron-oxygen species are also observed in carbonaceous materials where boron is used to enhance their oxidation stability through carbon active site poisoning, or, the formation of a boron oxide film on the surface [12-14]. Surface chemistry and structural characteristics of milled BC nanoparticles, produced in various atmospheres, have been investigated [15]. The material exhibited a more homogeneous structure and more spherical shape, and a negatively charged surface, possibly as a result of the formation of boronic groups, which may provide an attachment of silane and an increase of bond strength (Due to the presence of boric acid, which acts as a Lewis acid by accepting a hydroxyl ion, OH^-, forming a tetrahedral borate ion,

$B(OH)_4^-$) [15,16]. Other work reported the synthesis and thermal characterisation of poly-borosiloxanes (PBS) to be used as polymeric precursors for protection of carbon fibres in ceramic matrix composites. The PBS was obtained through the reaction of methyltriethoxysilane (MTES) or vinyltriethoxysilane (VTES) with boric acid in solution. FTIR spectra have showed that B-O-Si bonds exist in the structure and can be easily prepared [17]. Other studies have used silane agents to increase adhesion of epoxy adhesives on not to dissimilar materials to BC, such as silicon carbide (SiC) microparticles and nanoparticles [18,19].

2. Experimental materials and methods

2.1.Methodology

In an attempt to enhance our knowledge of silanes for the surface treatment of BC, this paper presents an experimental investigation into the relationships between various silane and corona-silane treatments, and the resulting mechanical performance and durability of BE-PMC subject to environmental exposure. In addition to the mechanical tests, a sintered BC block was used to assess the effect the various pre-treatments had on the wettability of BC. This provided better understanding of the treatment's influence on the viscosity of the uncured mixture, the density and porosity of the cured material and their influence on the short and long-term mechanical properties of the composite.

2.2.Materials

The materials used in the study were a 2-component epoxy adhesive, a wetting agent and BC. The BC powder consisted of a high-purity three-particle-size, which was added to the composite epoxy formulation. A square sintered block (PI-KEM Limited, Tamworth,

England) was used as a BC surface model to evaluate the surface chemistry. The adhesion promotion and surface modification to the BC was established through the use of a short carbon chain silane with an epoxy functional group (Fig. 1). The materials used for the composite are summarised in the Table 1.

2.3.Surface treatment

A γ-glycidyloxypropyl-trimethoxysilane (GPS) was used in an aqueous solution. Various studies have been conducted showing significant influence of the solution pH and silane concentration. Therefore, the optimum conditions for the silane solution were investigated using different pH values (3, 5, 7 and 9) and concentrations (0.5, 1 and 3 wt%). The pH solutions were prepared using deionised water (0.0 - 0.1 μS) and adjusted with acetic acid (10%vol) or sodium hydroxide (0.1 M), prior to the silane hydrolysis. The BC powder was immersed in fresh silane solutions (1 hour of hydrolysis, 550 rpm) for 30 minutes, followed by a drying time at 105C for 12 hours.

The use of corona (TANTEC HV 05-2) was considered both as a standard treatment and also prior to silane application to promote the formation of boron-oxygen species. The discharge (58 kJ/m^2) was applied on the BC inside thin PTFE envelopes (2 x 70 μm, one for each grit size) with an area of 210 x 145 mm^2. The discharge was applied seven times (forward ↔ backward) at a constant rate (~1.2 m/min) in each direction of the envelope and from side to side. In order to ensure a more effective treatment, the envelope was shaken every time that the direction or side was changed. The distance between the electrode and the envelope was kept constant, corresponding to a dielectric barrier thickness of 2.5 mm.

2.4.Manufacture process

Once exposed to the appropriate silane or plasma-silane treatment the BC particles were mechanically dispersed within the pre-heated adhesive and wetting agent using a Speedmixer

at 2700 rpm for 1 min., according to the mix ratios shown in Table 2. The mixture was then degassed, poured into stainless steel moulds (designed for the mechanical test specimens) and finally compacted under a force of 10 kN before a cure process at 40°C for 8 hours. Test specimens of the pure epoxy resin were also made for comparison.

2.5.Fourier Transform Infrared Spectroscopy

The characterisation of the material used in the composite and the surface chemical analysis of the untreated/silanised BC particles (7 – 1 μm) was carried out using a Perkin Elmer Spectrum 65 device with a deuterated triglycine sulfate detector (DTGS). The infrared spectra for the untreated and treated BC particles were obtained through transmittance and attenuated total reflectance mode (32 scans, 4 cm^{-1}) for the silane and adhesive's components. Also, a gel of the condensed silane was obtained using a high concentrated GPS aqueous solution (30%wt, pH5) and analysed with FTIR spectroscopy.

2.6.Surface free energy

Surface characterisation of the BC was performed using a semi-automated video KRUSS goniometer, and various probe liquids (deionised water, diiodomethane, and glycerol). A 5 μl liquid drop was deposited at a constant rate of 6.32 μl/minute on the sintered BC surface in order to the measure (age of 30 seconds, 7 - 9 measurements) the respective contact angle. The resulting experimental data were used in the van Oss, Chaudhury and Good equation (Eq. 1) to calculate surface free energy in terms of the dispersive and polar components [20]. Surface free energy components were also attained for the corona treated and silanised BC with respect to the pH value and concentration.

$$\gamma_L \cdot (1+\cos\theta) = 2 \cdot \left(\sqrt{\gamma_S^{LW} \cdot \gamma_L^{LW}} + \sqrt{\gamma_S^{+} \cdot \gamma_L^{+}} + \sqrt{\gamma_S^{-} \cdot \gamma_L^{-}} \right) \quad (1)$$

Where γ_L is the surface free energy at the liquid/vapour interface, γ_S is the surface free energy at solid/vapour interface, and θ is contact angle (CA). The superscripts *LW*, + and – are respectively the dispersive (LW, Lifshiz–van der Waals) and two polar (AB, Lewis acid and base interactions) components. The contact angle of the adhesive on the sintered BC block (θ_{exp}) was measured for comparison with the theoretical values determined using the surface free energy of the silanised BC and uncured adhesive using Eq. 2 [20].

$$\theta_T = \arccos\left[(2/\gamma_L)\cdot\left(\sqrt{\gamma_L^{AB}\cdot\gamma_S^{AB}}+\sqrt{\gamma_L^{LW}\cdot\gamma_S^{LW}}\right)-1\right] \quad (2)$$

In this case, γ_L is the surface free energy of the uncured adhesive, γ_S is the surface free energy of untreated or treated BC, θ_T is the theoretical contact angle of the adhesive on the BC surface, and superscripts *LW* and *AB* are the respective dispersive and polar ($\gamma^{AB} = 2\sqrt{\gamma^+\gamma^-}$) components. The surface free energy of the uncured adhesive (γ_L^{AB} = 0.01 mJ/m^2, γ_L^{LW} = 53.07 mJ/m^2) was obtained by measuring the contact angle on a series of substrates with known polar and dispersive components showed in the Table 3 (polyethylene, polycarbonate, polyvinylidene chloride, Zytel HTN, glass and BC).

2.7.Bulk density / Open porosity

The first physical property of the composite investigated was the bulk density (ρ_b, kg/m^3). This property is related to the density of the adhesive and BC, as well with their concentration in the formulation. However, the density of a high content BC composite with a specific particle size distribution and concentration depends also on its porosity (π_a, %), e.g. the amount of air trapped in the matrix, which is related to the adhesive's wettability on the BC surface and the actual processing of the composite (mix mode, temperature, degassing and pressure). This translates to (a) the adhesive's ability to replace the surrounding gas phase layer of the particle and (b) the mechanism by which a more uniform particle dispersion and

reduced air entrapment is achieved. The adhesive's ability to wet the BC depends on its surface chemistry, which can change when the BC is treated with silane solutions or plasma. Therefore, the bulk density ρ_b and open porosity π_a of the composite were measured according to BS EN 1389:2003 [21], using five test specimens (20 x 15 x 4 mm^3) per surface treatment and manufacture process. These properties were calculated from the following equations:

$$\rho_b = \frac{m_1}{m_3 - m_2} \cdot \rho_L \tag{3}$$

$$\pi_a = \frac{m_3 - m_1}{m_3 - m_2} \cdot 100 \tag{4}$$

Where m_1 is the mass of the dry test specimen, m_2 is the apparent mass of the immersed test specimen, m_3 is the mass of the soaked test specimen and ρ_L is the bulk density of the immersion liquid.

2.8.Scanning Electron Microscopy

Morphological studies of the untreated/silanised BC particles and the topography analysis of the fracture surface of the BC-epoxy composites were conducted to observe the effect of the surface treatment on the particles. The scanning electron microscopy (SEM) was performed with non-gold coated samples of the particles and composites through back scattering and secondary electrons using an Hitachi S-3400N and JEOL JSM-6480.

2.9.Mechanical Tests

The mechanical properties of the composite were obtained to evaluate whether or not the surface treatments were enhancing the adhesion between the BC and epoxy adhesive, using the various pH values and silane concentrations described above. Therefore, three mechanical

test methods were assessed using a universal testing machine unit (Nene Instruments Ltd, UK) and the test specimens described in Table 4 [22,23]. The test arrangements are shown in the Fig. 2.

The short beam three-point-bending method (3PB) is commonly used to evaluate the behaviour of brittle materials and composites under transverse load (static mode). In practice, this results in a contribution of both shear and tensile stress that depends on ratio between the span distance (s) and transverse area A, where w is the width of the specimen and h the depth) [24]. A high ratio (s/A >10) would provide more suitable information about the flexural properties of the material, whilst a low ratio (s/A = 4.5) would provide a shear dominant contribution (rupture strength, R_{tr}) that is calculated according to Eq.5.

$$R_{tr} = \frac{3 \cdot P \cdot s}{2 \cdot w \cdot h^2} \tag{5}$$

The composite tensile strength, t_{xy}, was obtained using the Iosipescu test. In this test, a failure was formed between the notch sections at 45° to the longitudinal axis of the beam (Fig. 3). This characteristic failure mode is generally observed with brittle-isotropic materials, and is the result of a pure tensile stress state located close to the notch tip [25,26]. This test was therefore used to determinate the tensile strength of the BC epoxy composite using Eq. 6.

$$t_{xy} = \frac{P}{w \cdot h} \tag{6}$$

A non-standard double v-notch (DVN) test, t, was used to evaluate shear strength, which was calculated according to Eq. 7.

$$t = \frac{P}{2 \cdot w \cdot h} \quad (7)$$

Where P is the maximum load observed during the test (N), w is the measured width of the test specimen (mm) and h is the measured height of the test specimen between the notch tips (mm). This provided a vertical crack, initiating from the notch tip.

3. Results and discussion

3.1.Fourier Transform Infrared Spectroscopy (FTIR) – BC Particles

Prior the evaluation of the different surface treatments BC (Fig. 4c), the spectra of the untreated particles (Fig. 4a) and non-hydrolysed/condensed GPS (Fig. 4b, 4d) were obtained.

The spectra of the untreated particles (Fig. 4a, Table 5) shows two strong characteristic bands at 1542 and 1074 cm^{-1}, which were attributed to the characteristic vibration modes of the central atom located in three-atom chain/diagonal (C–B–C) and B–C stretching of the icosahedral BC cell unit [27,28]. The broad form of the former can be consequence of other vibration modes (B–C, C–C and BC clusters) indicating the existence of more amorphous materials and higher disordered structures [28]. Also, the presence of free icosahedral B_{12} molecules is confirmed through a band located at 842 cm^{-1} [27]. Moreover, the bands at 3458 (broad), 1435 (strong) and 703-624 cm^{-1} (three, weak) were attributed to the O–H and B–O stretching and B–O–H deformation vibrations, respectively [28-30]. These bands give an indication that the untreated BC possesses hydroxyl groups and a native oxide layer on the surface, which may provide an attachment of the silane coupling agent (B–O–Si).

The non-hydrolysed silane (Fig. 4b) showed bands assigned to the aliphatic C–H stretching at 2942 and 2840 cm^{-1}, CH_2–O–CH_2 stretching at 1191 cm^{-1} and Si–O–CH_3 stretching at 1075 cm^{-1} and epoxy ring at 1254 and 909 cm^{-1} [31-34].

The silane gel (Fig. 4d, Table 5) exhibited an broad band at 3390 cm^{-1} as result of the presence of silanol group (Si–OH). The former was also confirmed with the vibration modes of the SiOH at 1646, 1091 and 907 cm^{-1}, confirming that the silane was fully hydrolysed using the pH5 aqueous solution [32,35]. The increase of intensity of band at 1091 cm^{-1} is congruent with the higher absorbance showed by the other vibration modes attributed to the silanol group. Additionally, the condensation reaction was observed with the appearance of a strong band at 1008 cm^{-1}, which was assigned to the Si-O-Si stretching of the cross-linked silane as an outcome of the high GPS concentration used to obtain the gel. A weak band located at 1724 cm^{-1} was assigned to carbonyl group (C=O) stretching vibration as result of the oxidation of the epoxy group and consequent opening of the ring [31]. This degradation process led to a decrease in the number of epoxy rings (1252 cm^{-1}) available to react with the adhesive, which may result in a lower effectiveness of the silane treatment.

To better understand the effect of the various silane treatments on the surface of the BC, the spectra of the silanised particles were acquired with respect to the solution pH and GPS concentration (Fig. 4c, Table 5). The solution pH clearly showed an influence on the surface chemistry of the treated BC. The treatment with pH3 solution was less pronounced, mostly as a consequence of the lower stability of the hydrolysed silane in more acidic solutions. The silane treatment was more evident with pH5 and pH7, which can be related to the presence of a more monomeric silanol aqueous solution as a result of a faster hydrolysis and slower condensation of the silane in milder acidic conditions, promoting greater stability of the hydrolysed compound [33,34]. Beyond pH7 the surface chemistry changes were less pronounced, which is commonly related to the presence of dimers or larger oligomers and a decreased number of silanol groups available to react with the hydroxyl groups on the BC surface (as result of the rapid condensation of the silane in the more basic solutions). The GPS concentration also affects the number of silanol groups available to react to the surface, and the extension of the condensation process through silane cross-linking and/or the formation of

bonds on the ceramic surface. These can be confirmed in the Fig. 5 by the intensity increase of the bands attributed to the silanol vibration modes (3669–3638, 1151 and 964 cm^{-1}) and Si–O–Si stretching (1075 cm^{-1}) with the increment of silane concentration using pH5 and pH7 solutions [35-37]. Finally, multiple bands of medium (1392–1382 and 968–942 cm^{-1}) and lower (684–675 cm^{-1}) intensity were found on the surface of the BC silanised with pH7 solution, which was attributed to the stretching and bending vibrations of the borosiloxane bond (B–O–Si) [38-40].

3.2.Scanning Electron Microscopy (SEM) – BC Particles

The BC particles generally exhibited smooth, rippling and gradual concentric fractures (conchoidal), which are normally observed in brittle materials exhibiting little or no cleavage. Small fissures were also observed propagating outwards from the centre of the fractures. The F60 and F360 showed a greater extent of this type of fractures (Fig. 6a, 6b), whilst the F1200 tended to exhibit more rounded, polygonal-type shapes with less sharp edges as result of faceted fractures (Fig. 6c). This difference of morphology may be related to the milling process used to obtain the smaller particle size. To summarise, most of the particles possessed a plate-like shape with relatively sharp, thin edges that may act as crack promoters. Thus, the BC particles morphology could also affect the mechanical properties of the composite.

Elemental analysis showed a boron/carbon ratio higher than that expected from the stoichiometry of the BC (4:1). This was not unexpected given the possible substitution of the two elements in the C-B-C chain linked to $B_{11}C$ icosahedra clusters, located along the main diagonal of the BC rhombohedral structure. Therefore, the higher ratio could be the result of the presence of regions of β-rhombohedral boron [15,27,30]. The untreated BC particles exhibited a small amount of contamination, confirmed by the noticeable lighter spots visible in Fig. 6d using back scattering electron analysis. These result from higher atomic number elements, such as iron, silicon and oxygen from silicates, carbonates and iron or boron oxides.

Also, the silanised ceramic material showed a lighter surface and smoother edges as result of interaction of the electrons with the silane layer (Fig. 6c).

3.3.Surface free energy

The surface free energy of the untreated BC was 52.5 mJ/m^2, exhibiting a high dispersive component (γ_S^{LW} = 33.7mJ/m^2). These values are in agreement with reported surface free energy values for BC coated materials [41]. The Lewis acid is the higher polar component (γ_S^+ = 16.5 mJ/m^2) probably as a result of the presence of boron-oxide species. It was these native oxygen-containing species that were expected to provide a means of attachment to the silane coupling agent to form a covalent bond (B-O-Si) on the BC surface. The BC with corona treatment exhibited an increase in the surface free energy to 64.6 mJ/m^2 as a consequence of a higher Lewis acid component (γ_S^+ = 44.8mJ/m^2). Hence, a decrease of the contact angle was observed with more polar liquids, e.g. water dropped from 47º to 7.5º. The higher Lewis acid nature can be related to the presence of negatively surface-charged boronic groups. Some species of boronic acids (R-B(OH)$_2$) have been reported to accept an hydroxyl ion to form a tetrahedral borate ion [15-17]. The effect of pH solution and silane concentration on the surface free energy of the BC was also investigated in terms of their dispersive, Lewis acid and base (Fig. 7, Table 6) components. The silanised BC exhibited a lower surface free energy, depicted by a decrease of the Lewis acid component from 16.5 to 2.1 mJ/m^2. Thus, higher angles for the polar liquids were observed as a result of the hydrophobic nature of the organic functional groups present on the GPS layer, leading to an increase in the water contact angle from 51º to 85°. On the other hand, the dispersive component increased from 33.7 to 38.7 mJ/m^2, particularly when lower pH values (3 and 5) and higher concentrations (1% and 3% wt.) were employed. This led to a decrease in contact angle for the pure dispersive liquid (diiodomethane) from 51º to 42°.

Notably, the surface free energy changes observed with the silanised BC were likely to affect the adhesive's wettability. To confirm this statement, the contact angle of the uncured adhesive on silanised BC was measured using 3% GPS solution with the different pH values. The experimental contact angles on the untreated and treated substrates were compared with the theoretical values (Table 7) using the surface free energy components of the untreated/treated BC substrates and uncured epoxy adhesive (γ_L^{AB} = 0.01 mJ/m^2, γ_L^{LW} = 53.07 mJ/m^2).

The theoretical values show good agreement with the measured adhesive contact angle according to a particular treated/untreated surface. Thus, the silanised BC demonstrated some evidence of an outward orientation of the epoxy functional groups from the surface of the BC leading to an increased hydrophobicity and improved adhesive wettability. This surface property change could then be directly related to the compound uncured viscosity, the resulting density/porosity of cured material and subsequently the performance and durability of the BE-PMC.

3.4.Bulk Density / Open Porosity

The epoxy and BC exhibited a density of 1.12 g/cm^3 and 2.52 g/cm^3, receptively (Fig. 8a). These values are in agreement with the data showed in literature and respective technical data sheets. The theoretical value calculated for 80% wt. of BC is 2.24 g/cm^3.

The experimental density of the BE-PMC was lower than the expected theoretical value, ranging from 1.76 to 2.01 g/cm^3 (Fig. 8a, 8b), with the lowest density being that of the original composite. An improved manufacturing process with a high shear rate mix method degassing resulted in a small increase to 1.90 g/cm^3 (untreated). This confirms a better dispersion/lower agglomeration of the particles in the epoxy matrix and less air voids [42-44]. The highest values were achieved with either the silane (1.93 - 1.99 g/cm^3) or corona (1.99 g/cm^3) treated BC particles. The density for the silanised composites was higher when lower

concentrations (0.5 - 1.0%) and pH3-5 were used. The difference between the experimental and theoretical values suggests a porous structure, which was confirmed with the open porosity values (Fig. 9). As to be expected, the sintered BC specimen displayed porosity whilst the adhesive showed some "water absorption" as a result of possessing a more or less open three-dimensional structure (0.56%). In the case of the BE-PMC, the highest porosity was observed with the original (1.34%) composite. The use of the refined manufacturing process led to a steep decrease of the porosity from 1.34 to 0.34% (untreated). Notably, the lowest porosity was displayed by the treated composites, especially the corona treated (0.15%) particles. The majority of the silanised composites exhibited porosities between 0.22 and 0.26%. The only exception is observed for BC treated with a pH3 solution and 3% concentration, exhibiting porosity respectively of 0.11%. This result was thought to be related to the higher wettability observed in the sessile drop method for the treated BE-PMC, e.g. the existence of a more intimate contact between the two materials resulted in a mixture with lower viscosity and a composite with reduced voids.

3.5.Mechanical testing

The following mechanical data was acquired to assess any improvements in shear, tensile and mix-mode performance as a result of the various surface treatments effect on the adhesion between the BC and epoxy adhesive. For comparison, the strength of pure epoxy resin was obtained using the same test methods to better understand the properties of the binder and the effect of adding the BC in the polymeric matrix. The following data doesn't provide sufficient information for statistical analysis but gives some indication about the relative influence of the surface treatments used in this study.

3.5.1. Rupture strength

The rupture strength of the epoxy adhesive and composites at room temperature are shown in Fig. 10a. The addition of 80% BC in the polymeric matrix led to a significant 44% decrease in rupture strength, in comparison to the pure epoxy resin (i.e. from 93 to 52 MPa). The high shear rate mix method and degassing process used in the untreated composite resulted in a strength increment of 25% (65 MPa). The corona treatment demonstrated an improvement in strength of 8% as compared to the untreated. The silane treatment provide the most significant improvement, obtaining a rupture strength of 82 MPa (88% of the of the bulk resin strength). To better understand the effect of the various silane treatments on the mechanical properties of the composite, the rupture strength is presented with respect to the pH solution and silane concentration (Fig. 10b). The solution pH clearly demonstrated a significant influence on the mechanical properties of the composite. The pH3 solution was detrimental, most likely due to the lower stability of the hydrolysed silane in more acidic solutions. Strength was generally improved with pH7 solution, supporting an earlier finding reported in literature [7,33]. Beyond pH7 the improvements were lost with the highest silane concentration (3%GPS), thought to be related to the elimination of the reactive silanol groups and the presence of more dimers, trimers or even larger oligomers as result of a faster silane condensation in the presence of more basic solutions [34]. This suggests the formation of a highly condensed silane layer with fewer covalent bonds available for attachment to the surface, which consequently led to the detriment of the adhesion between the epoxy and BC particles. The silane concentration also had a marked effect on the strength according to solution pH. The best performance was observed using 0.5 - 1.0%GPS, with the exception of the pH3 solution. Beyond 1.0% the strength was reduced, this time with the exception of solution pH7. Together, these results show a strong influence of the solution pH and concentration on the transverse rupture strength of the composite. The optimum treatment conditions to achieve the best mechanical properties for the composite are 0.5 - 1.0% of silane in a pH5 - 7 solution. The use of corona prior to the silane treatment resulted in a small decrease of the strength.

3.5.2. Tensile strength

The tensile strength of the bulk epoxy resin and BE-PMCs at room temperature are shown in Fig. 11a. The addition of 80% BC in the resin led to a significant decrease in tensile strength of 57% (i.e. from 48 MPa to 20 MPa). The untreated composite developed a higher strength (39 MPa) as a result of the more refine manufacturing process. The corona treatment demonstrated a small improvement of 8% to 42 MPa. The best of the silane treatments exhibited equivalent strength to that of the bulk epoxy resin. These improvements varied according to the particular silane treatment, as can be seen in Fig. 11b. Most pH solutions provided some improvement in the tensile strength. The higher values were generally observed with pH5 and pH7 solutions, following similar reasoning as reported in the previous section. Nevertheless, some exhibited lower strengths when formulated with pH3 and pH9 solutions. This was specifically observed for the 3% GPS solutions, highlighting a strong relationship with silane concentration. The better performances were formed using 0.5% and 1.0% GPS for a specific pH. The exception was solution pH7, which exhibited a more consistent strength through every concentration. Thus, the tensile strength was again affected by the solution pH and concentration, exhibiting optimal conditions when 0.5% to 1.0% GPS were used in pH5 and pH7 solutions. The corona treatment applied on the BC prior to the silane again results in a small decrease in strength.

3.5.3. Shear strength

The shear strength of the epoxy adhesive and composites acquired through a non-standard test are shown in the Fig. 12a. The addition of the BC particles led to a steep decrease in shear strength (71%) from 31 to 9 MPa (original). The use of the high shear rate mechanical mix method and degassing in the stage of the processing had no effect in strength of the composite (untreated). An improvement of 25% and 56% is observed when corona (11 MPa) and GPS

treatment (14 MPa) was applied to the BC particles respectively. The evaluation of the shear strength was also conducted for the silanised BC particles using different pH values and concentrations (Fig. 12b). Although all silane treatments led to an increase of the strength, the pH7 and pH9 solutions were the ones showing the greatest improvements. The highest values for a specific solution are observed using 0.5 - 1.0% of GPS, especially between pH5 and pH7 values. The best treatment conditions were 0.5 - 1.0% of silane in a pH7 solution. The corona treatment prior to silane treatment again demonstrated a small reduction in strength.

3.6.Scanning Electron Microscopy (SEM) – Composite Failure Surfaces

The fracture of all species generated a rough topography typical of high filler content brittle polymeric matrix composites, possessing particles with angular shapes and sharp edges.

The high void content in the original and untreated specimens (Fig. 13a, 13b) was the result of the entrapped air introduced during the mix and moulding stage of manufacture. The original process was performed under conditions open to atmosphere mixed with a z-blade mixer (Fig. 13a). The poor strength of the original composite (Fig. 10a, 11a, 12a) can be interpreted from the fracture mechanism shown in 13b, which produced a weak brittle failure resulting from poor mechanical strength of the highly porous matrix (Fig. 9).

The improved but untreated BE composite exhibit lower porosity (Fig. 13c) as result of the combined high shear rate mix method, degassing before moulding and high pressure loading before curing. Given the high of BC content and relatively low viscosity of the resin used in previous findings, the displacement of the particles from the surface by entrapped air as result of the high density of BC or agglomeration of the particles in the epoxy matrix [4] were not replicated. These specimens exhibited crack branching and deflection around the particles (Fig. 13b, 13d), which resulted in a higher strength.

In contrast, the silane and corona treatments on BC led to a visible decrease in the amount of trapped air voids (Fig. 13e, 13g). In the case of the corona treatment this is likely to be the

result of improved wetting due to a substantial increase in the total surface free energy (Fig. 6). In the case of the silanised composite, it is more likely to be due to a combination of a higher dispersive interaction between the BC and epoxy (Fig. 6, Table 7) and reduced viscosity of the compound from the better dispersion of the particles in the resin (lower standard deviation, Fig. 8)

Further evaluation was conducted to provide indication of the failure modes on the surface of individual BC particle in the matrix of the treated composite (Fig. 13f, 13h). The improved strength provided by the corona treatment appears to be the result of a better adhesion, showing traces of resin on the surface of some large particles, apparently as a consequence of cohesive adhesive failure at the BC-epoxy interface (Fig. 13f). Even better adhesion resulted from the silanised composite, exhibiting distinct regions of epoxy and small BC particle clusters, again, remaining attached to surface of the larger particles (Fig. 13h). The silane treatment appears to provide a stronger bond compared to that of the corona treated BC surface. This may be related to the chemical modification of the surface and consequent intermolecular interaction mechanisms between the BC particle and epoxy resin. Hence, more advance techniques must be conducted, such as X-ray photoelectron spectroscopy (XPS) and secondary ion mass spectrometry (SIMS), to provide more evidence of a potential chemical bonding.

4. Conclusions

This study investigated the application of a silane coupling agent to improve the adhesion between a two component epoxy resin and BC. Initial surface analysis confirmed the presence of hydroxyl groups and B-O bonds on the untreated BC particles. This provided evidence of suitable functional groups for the attachment of a silane coupling agent. Corona treatment was also considered prior to silanisation to further promote the formation of boron-oxygen

species. This resulted in an increased surface free energy, essentially as result of a higher polar component, which was assumed to be from the formation of boron–oxygen species on the surface.

Silane modification of the BC was found to be most effective using mild acidic and neutral solutions (pH5 and pH7) assumed to be the result of the greater stability of the hydrolysed silane and the presence of a more monomeric silanol aqueous solution. The silanised surface exhibited a small gain in its dispersive energy component but a significant reduction in its polar component, as a likely consequence of the hydrophobic nature of the formed GPS layer on the BC. The former provided better adhesive wettability and more effective dispersion of the particles in the epoxy matrix, leading to a composite with higher density and lower porosity.

Mechanical testing demonstrated correlations between strength improvement and the various surface modifications and physical characterisation. Untreated control specimens generally exhibited poor adhesion between the BC and epoxy resin. The use of the corona treated BC led to an increase in the BC-epoxy composite strength ranging between 8% and 25%. This was accompanied by fracture surfaces exhibiting resin layers with particles visibly attached to the surface. The most improved mechanical properties were however obtained by the BC-epoxy composite treated with silane only, exhibiting strength increases ranging between 24% and 56%. Similar flexural and tensile strengths to that of the pure epoxy were achieved but at best only 40% of the adhesive's shear strength was obtained. The higher bond strength compared to the untreated specimens was confirmed with the presence of easily distinguishable layers of epoxy and small particle clusters remaining attached to the BC particles.

Acknowledgments

This work was carried out within the scope of a PhD research project funded by Oxford Brookes University. Also, the authors wish to acknowledge the assistance of Advance Materials Group from Science Technology Foundation Council (STFC) and Department of Biological and Medical Sciences from Oxford Brookes University (OBU) for providing materials and SEM infrastructure, respectively.

References

[1] F. Thévenot, Boron carbide—a comprehensive review, J. Eur. Ceram. Soc. 6, no. 4 (1990) 205-225.

[2] B. Suresha, G. Chandramohan, M.A. Jawahar, S. Mohanraj, Three-body abrasive wear behavior of filled epoxy composite systems, J. Reinf. Plast. Compos. 28, no. 2 (2009) 225-233.

[3] S. Canfer, S. Robertson, Method for Manufacturing Composite Articles Containing Boron Carbide, U.S. 2010/0041808 A1, 2010.

[4] J. Abenojar, M.A. Martínez, F. Velasco, V. Pascual-Sanchez, J.M. Martin-Martinez, Effect of boron carbide filler on the curing and mechanical properties of an epoxy resin, J. Adhes. 85, no. 4-5 (2009) 216-238.

[5] R.E. Sund, R.B. Walton, Gamma Rays from Short-Lived Fission-Fragment Isomers, Phys. Rev., no.3, vol.146 (1966) 824-835.

[6] C.H. Lee, J. Park, B.H. Choi, H. Oh, Y.S. Han, Development of Neutron Shielding Block by Epoxy Molding, Korea Atomic Energy Research Institute, Taejon, Republic of Korea, 2001.

[7] E.P. Plueddemann, Silanes Coupling Agents, 2nd Edition, Plenum Press, New York, 1991.

[8] M-L. Abel, R.D. Allington, R.P. Digby, N. Porritt, S.J. Shaw, J.F. Watts, Understanding the relationship between silane application conditions, bond durability and locus of failure, Int. J. Adhes. Adhes. 26, no. 1 (2006) 2-15.

[9] J.G. Matisons, Silane Coupling Agents and Glass Fibre Surfaces: A Perspective, Silanes and Other Coupling Agents 5 (2009) 3-22.

[10] K.L. Mittal (Ed.), Silanes and other coupling agents 3, VSP, Utrecht, 2003.

[11] N. Brack, A.N. Rider, B. Halstead, P.J. Pigram, Surface modification of boron fibres for improved strength in composite materials, J. Adhes. Sci. Technol. 19, no. 10 (2005) 857-877.

[12] P. Ehrburger, P. Baranne, J. Lahaye, Inhibition of the oxidation of carbon-carbon composite by boron oxide, Carbon 24, no. 4 (1986) 495-499.

[13] S. Labruquère, H. Blanchard, R. Pailler, R. Naslain, Enhancement of the oxidation resistance of interfacial area in C/C composites. Part I: oxidation resistance of B–C, Si–B–C and Si–C coated carbon fibres, J. Eur. Ceram. Soc. 22, no. 7 (2002) 1001-1009.

[14] Y-J. Lee, H-J. Joo, L.R. Radovic, Preferential distribution and oxidation inhibiting/catalytic effects of boron in carbon fiber reinforced carbon (CFRC) composites, Carbon 41, no. 13 (2003) 2591-2600.

[15] M.W. Mortensen, P.G. Sørensen, O Björkdahl, M.R. Jensen, H.J.G. Gundersen, T. Bjørnholm, Preparation and characterization of Boron carbide nanoparticles for use as a novel agent in T cell-guided boron neutron capture therapy, Appl. Radiat. Isot. 64, no. 3 (2006) 315-324.

[16] S. Goldberg, S.M. Lesch, D.L. Suarez, Predicting boron adsorption by soils using soil chemical parameters in the constant capacitance model, Soil Sci. Soc. Am. J. 64, no. 4 (2000) 1356-1363.

[17] R.L. Siqueira, I.V.P. Yoshida, L.C. Pardini, M.A. Schiavon, Poly(borosiloxanes) as precursors for carbon fiber ceramic matrix composites, Mater. Res. 10, no. 2 (2007) 147-151.

[18] J. Abenojar, J.C. Del Real, M.A. Martinez, M.C. Santayana, Effect of silane treatment on SiC particles used as reinforcement in epoxy resins, J. Adhes. 85, no. 6 (2009) 287-301.

[19] T. Zhou, X. Wang, G.U. Mingyuan, X. Liu, Study of the thermal conduction mechanism of nano-SiC/DGEBA/EMI-2, 4 composites, Polymer 49, no. 21 (2008) 4666-4672.

[20] C.J. van Oss, Use of the combined Lifshitz–van der Waals and Lewis acid–base approaches in determining the apolar and polar contributions to surface and interfacial tensions and free energies, J. Adhes. Sci. Technol. 16, no. 6 (2002) 669-677.

[21] BS EN 1389:2003, Advanced technical ceramics - Ceramic composites – Physical properties - Determination of density and apparent porosity, 2003.

[22] BS EN ISO 3325:1999, Sintered metal materials, excluding hardmetals – Determination of transverse rupture strength, 1999.

[23] BS EN 12289:2005, Advanced technical ceramics – Mechanical properties of ceramic composites at ambient temperature – Determination of in-plane shear properties, 2005.

[24] A.A. Roche, J. Dumas, J.F. Quinson, M. Romand, in: D. Baptiste (Ed.), Mechanics and mechanisms of damage in composites and multi-materials, ESIS Publication 11 (1991) 269.

[25] L.G.B. Manhani, L.C. Pardini, F.L. Neto, Assessment of tensile strength of graphites by the Iosipescu coupon test, Mater. Res. 10, no. 3 (2007) 233-239.

[26] J.R.M d'Almeida, S.N. Monteiro, The Iosipescu test method as a method to evaluate the tensile strength of brittle materials, Polym. Test. 18, no. 6 (1999) 407-414.

[27] D. Ghosh, G. Subhash, C.H. Lee, Y.K. Yap, Strain-induced formation of carbon and boron clusters in boron carbide during dynamic indentation, Appl. Phys. Lett. 91, no. 6 (2007) 061910-061910.

[28] M.G. Rodríguez, O.V. Kharissova, U. Ortiz-Méndez, Formation of boron carbide nanofibers and nanobelts from heated by microwave, Rev. Adv. Mater. Sci. 7, no. 1 (2004) 55-60.

[29] M. Kakiage, Y. Tominaga, I. Yanase, H. Kobayashi, Synthesis of boron carbide powder in relation to composition and structural homogeneity of precursor using condensed boric acid–polyol product, Powder Technol. 221 (2012) 257-263.

[30] S. Mondal, A.K. Banthia, Low-temperature synthetic route for boron carbide, J. Eur. Ceram. Soc. 25, no. 2 (2005) 287-291.

[31] C.M. Bertelsen, F.J. Boerio, Linking mechanical properties of silanes to their chemical structure: an analytical study of γ-GPS solutions and films, Prog. Org. Coat. 41, no. 4 (2001) 239-246.

[32] B.B. Johnsen, K. Olafsen, K., A. Stori, Reflection-absorption FT-IR studies of the specific interaction of amines and an epoxy adhesive with GPS treated aluminium surfaces, Int. J. Adhes. Adhes. 23, no. 2 (2003) 155-163.

[33] A.A. Parker, J. Maclachlan, The relationship between silane hydrolysis and polymer adhesion to glass as studied by 13C solid state NMR, Silanes and Other Coupling Agents 2 (2000) 27-40.

[34] G. Xue, J.L. Koenig, H. Ishida, D.D. Wheeler, Chemical reactions of an epoxy-functional silane in aqueous solutions, Rubber Chem. Technol. 64, no. 2 (1991) 162-171.

[35] D.G. Kurth, G.K. Broeker, C.P. Kubiak, T. Bein, Surface attachment and stability of cross-linked poly (ethylenimine)-epoxy networks on gold, Chem. Mater. 6, no. 11 (1994) 2143-2150.

[36] A.N. Rider, Factors influencing the durability of epoxy adhesion to silane pretreated aluminium, Int. J. Adhes. Adhes. 26, no. 1 (2006) 67-78.

[37] W.S. Hanoosh, E.M. Abdelrazaq, Polydimethyl siloxane toughened epoxy resins: tensile strength and dynamic mechanical analysis, Malaysian Polym. J. 4, no. 2 (2009) 52-61.

[38] R. Mansour, M. Lafjah, F. Djafri, A. Benguedda ch, Synthesis of borosilicate zeotypes by steam-assisted conversion method, J. Korean Chem. Soc. 51, no. 2 (2007) 178-185.

[39] A. Wróblewska, A. Fajdek, E. Milchert, B. Grzmil, The Ti-MWW catalyst-its characteristic and catalytic properties in the epoxidation of allyl alcohol by hydrogen peroxide, Polish J. Chem. Technol. 12, no. 1 (2010) 29-34.

[40] J-B. Orhan, V.K. Parashar, J. Flueckiger, M.A.M. Gijs, Internal modification of poly (dimethylsiloxane) microchannels with a borosilicate glass coating, Langmuir 24, no. 16 (2008) 9154-9161

[41] M.F. Maitz, R. Gago, B. Abendroth, M. Camero, I. Caretti, U. Kreissig, Hemocompatibility of low-friction boron–carbon–nitrogen containing coatings, J. Biomed. Mater. Res., Part B 77, no. 1 (2006) 179-187.

[42] H.R. Dennis, D.L, Hunter, D. Chang, S. Kim, J.L. White, J.W. Cho, Nanocomposites: The importance of processing, Plast. Eng. 57, no. 1 (2001) 56-57.

[43] Wang, Q., Xia, H., & Zhang, C. (2001). Preparation of polymer/inorganic nanoparticles composites through ultrasonic irradiation. *Journal of applied polymer science*, *80*(9), 1478-1488.

[44] Rodgers, R. M., Mahfuz, H., Rangari, V. K., Chisholm, N., & Jeelani, S. (2005). Infusion of SiC Nanoparticles Into SC-15 Epoxy: An Investigation of Thermal and Mechanical Response. *Macromolecular Materials and Engineering*, *290*(5), 423-429.

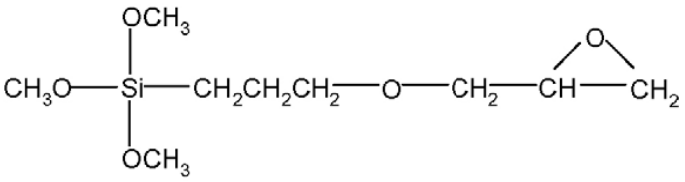

Fig. 1. γ-glycidyloxypropyl-trimethoxysilane (GPS) molecule structure before hydrolysis.

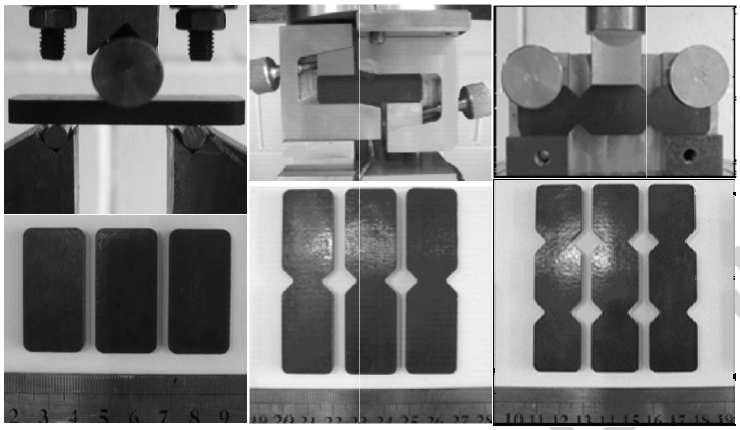

Fig. 2. Test arrangements employed for the (a) three-point bending (b) Iosipescu and (c) double-v notch.

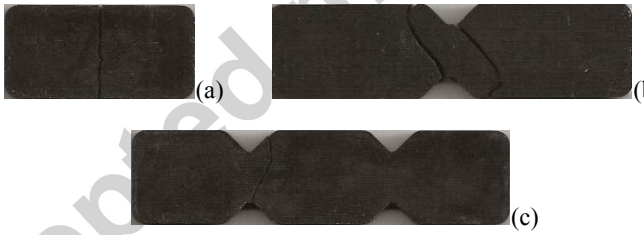

Fig. 3. Characteristic failure modes of the epoxy composite for the (a) three point-bending, (b) Iosipescu and (c) double v-notch test methods.

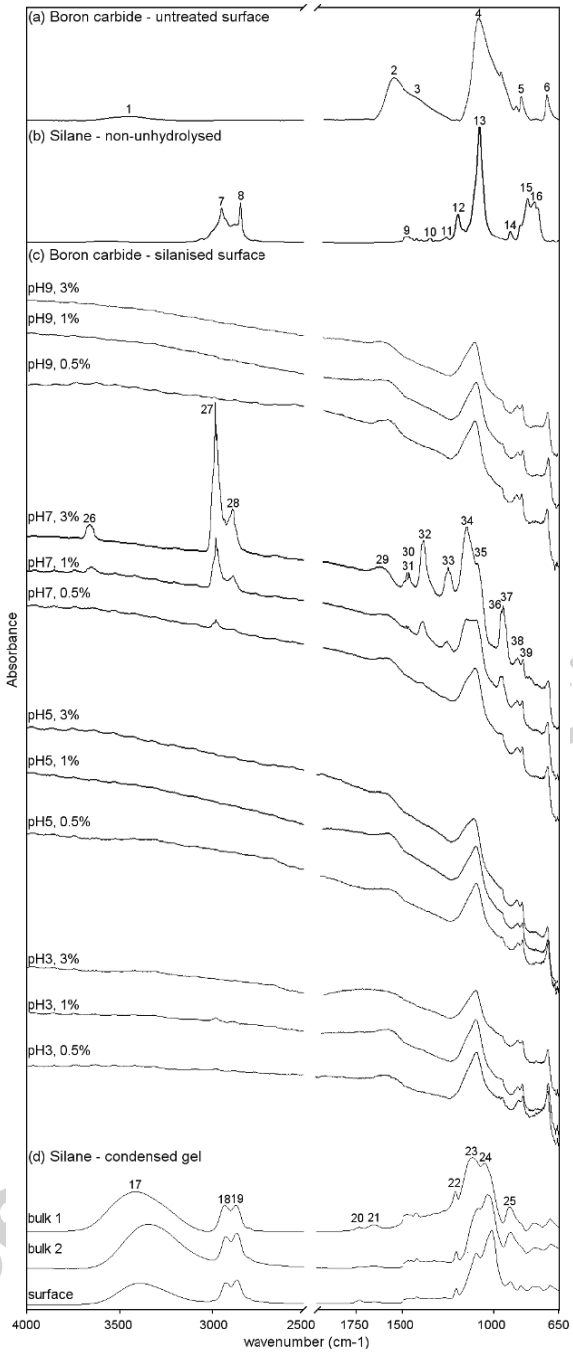

Fig. 4. FTIR spectra of the (a) untreated boron carbide, (b) unhydrolysed silane, (c) treated boron carbide and (d) silane condensed gel

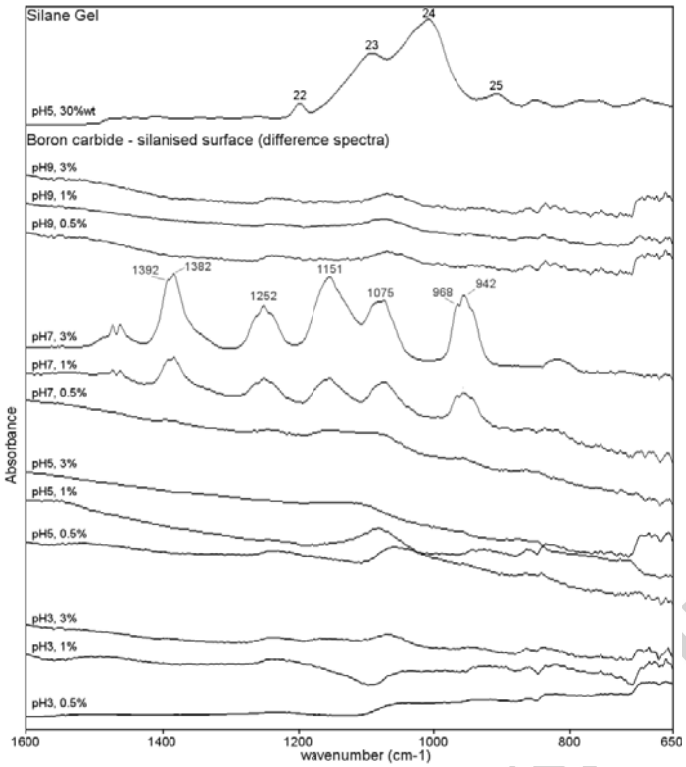

Fig. 5. FTIR fingerprint region of the (a) silane gel spectra and (b) difference spectra between the silanised and untreated boron carbide surface

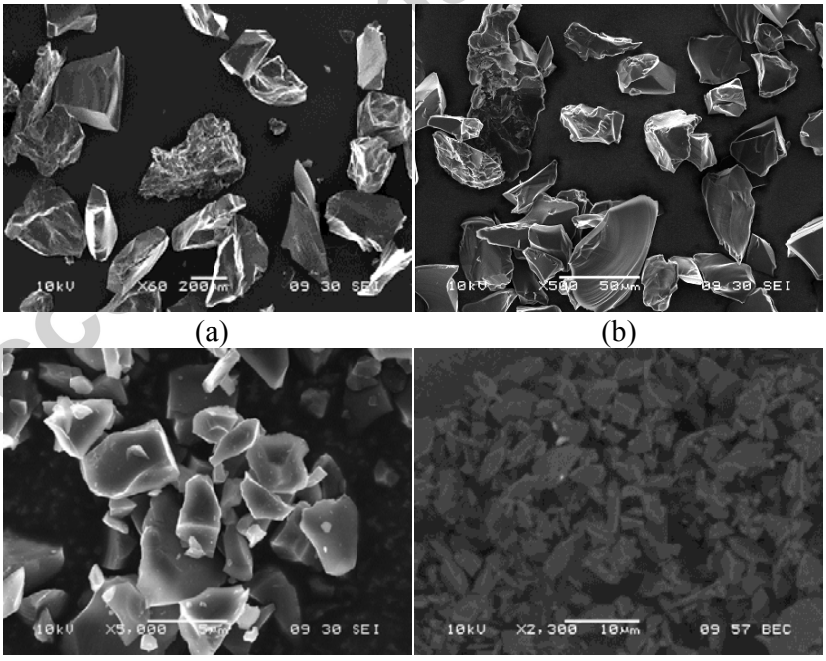

(a) (b)

(c) (d)

Fig. 6. Scanning electron microscopy with secondary electrons, SE, on (a) F60 (b) F360 and (c) F1200 and with back scattering electrons, BSE, on (d) F1200.

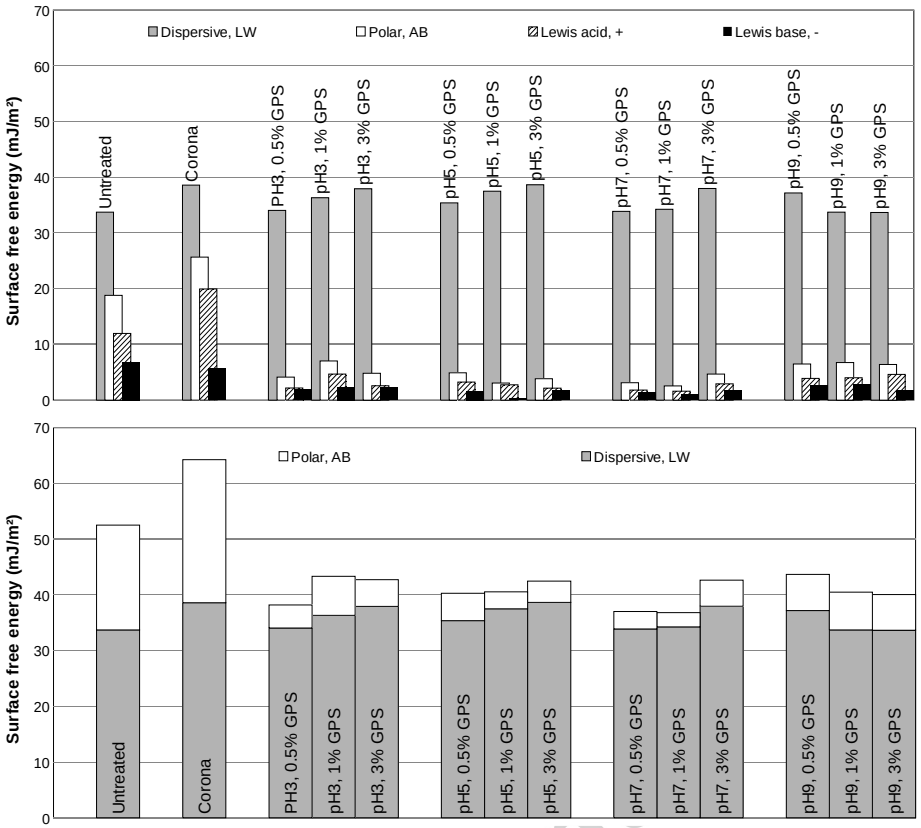

Fig. 7. Surface free energy values for different pH and silane concentrations.

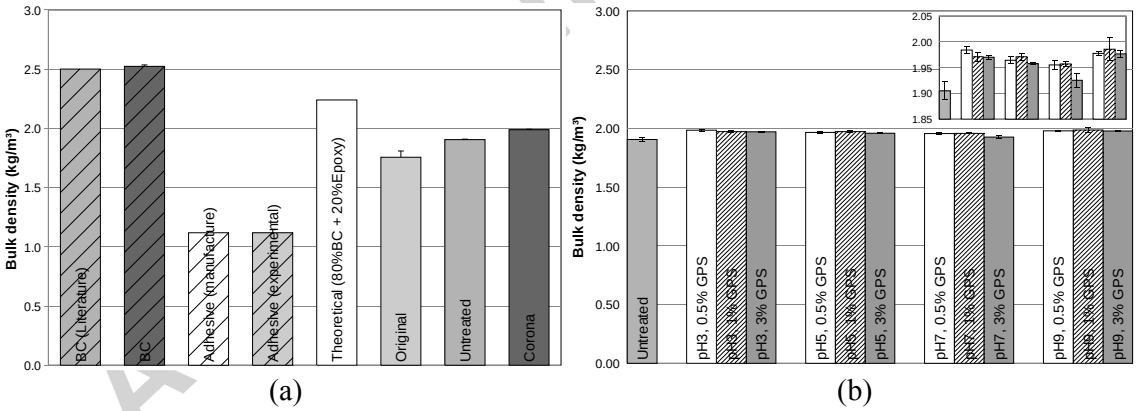

(a) (b)

Fig. 8. Experimental and theoretical values of bulk density obtained for the (a) boron carbide, epoxy adhesive and original/untreated/corona treated composite (b) untreated and silanised composite with different pH values and concentrations.

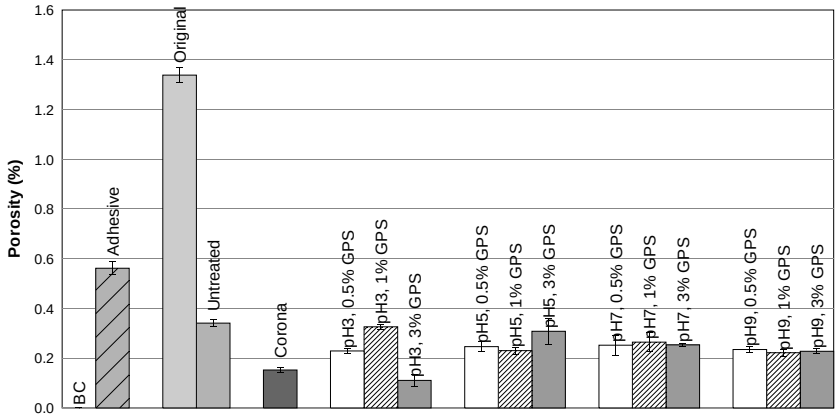

Fig. 9. Porosity of the boron carbide, epoxy adhesive and the different composites.

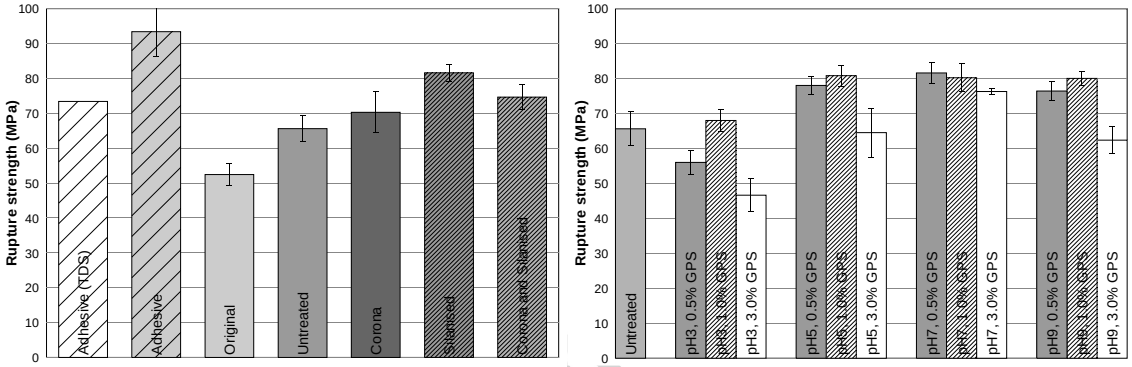

(a) (b)

Fig. 10. Rupture strength of (a) epoxy adhesive and of the original, untreated, corona treated, silanised and corona and silane treated composite (b) silanised composite with various pH values and concentrations.

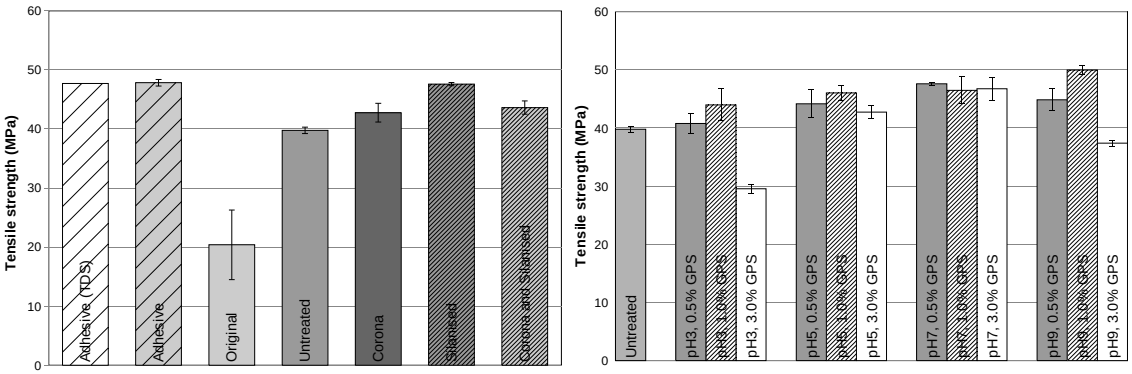

(a) (b)

Fig. 11. Tensile strength of (a) epoxy adhesive and of the original, untreated, corona treated, silanised and corona and silane treated composite (b) silanised composite with different pH values and concentrations.

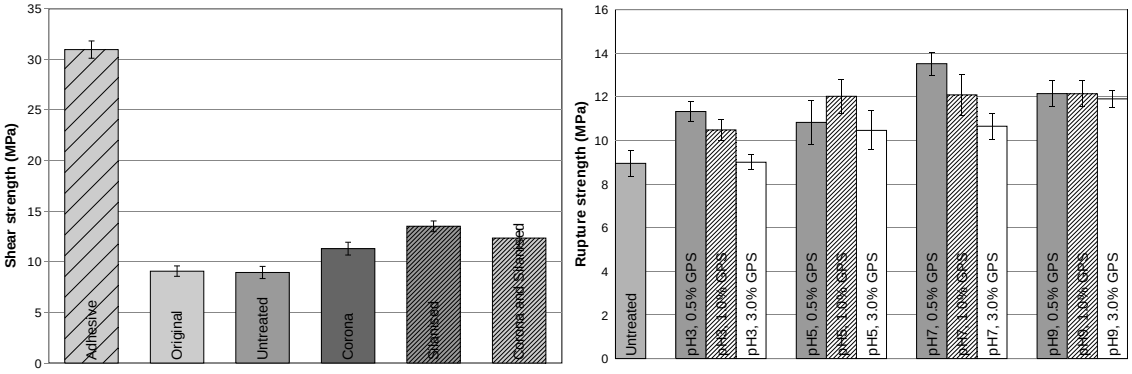

(a) (b)

Fig. 12. Shear strength of (a) epoxy adhesive and of the original, untreated, corona treated, silanised and corona and silane treated composite (b) silanised composite with different pH values and concentrations.

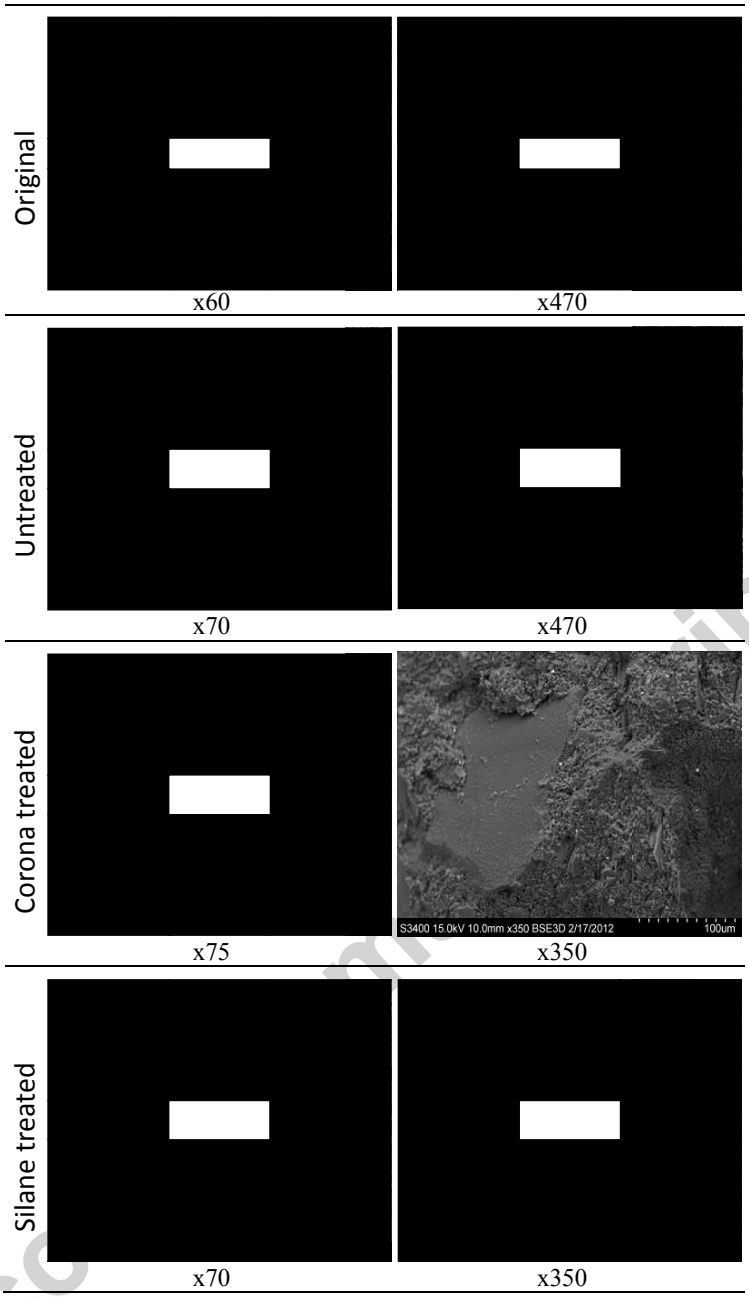

Fig. 13. SEM micrographs using back scattering electrons on the composite failure surfaces.

Table 1 Reference and description of the materials.

Material	Reference	Description
Epoxy adhesive	Bitrez CPR600	Bisphenol-A epichlorohydrin resin, MW < 700
	Air Products Ancamide 506	Fatty acids, tall-oil reaction products with tetraethylenepentamine (TEPA) and 3,6,9-triazaundecamethylenediamine
Wetting agent	BYK-W980	2-butoxyethanol and polyamine amide salt
Boron carbide	Pi-Kem, F1200/F360/F60	Particles, 7 – 1 μm, 40 – 12 μm, 300 – 212 μm
	Pi-Kem, 009XP9258	Sintered samples, 12 x 25 x 6 mm^3
Silane	Aldrich 440167	γ-glycidyloxypropyl-trimethoxysilane (GPS), 98%

Table 2 Ratios of the materials used for the manufacture of the composite.

Material	Ratio (wt%)
Adhesive (resin / hardener)	12.9 / 7.0
Wetting agent	0.3
Boron carbide particles (F60 / F360 / F1200)	19.3 / 21.9 / 39.6

Table 3 Contact angles of the probe liquids and surface free energy obtained for various substrates

Substrate	Contact angle (º, degrees)			Surface free energy (mJ/m^2)			
	H_2O	CH_2I_2	$C_3H_8O_3$	γs^{LW}	γs^{AB}	γs^{+}	γs^{-}
Polyethylene	95.6 ± 0.9	51.4 ± 1.3	76.6 ± 1.8	33.5	0.7	0.3	0.4
Polycarbonate	75.0 ± 1.7	29.5 ± 1.7	58.8 ± 0.3	44.4	3.1	4.9	0.5
Polyvinylidene Chloride	68.8 ± 2.1	30.3 ± 1.5	53.4 ± 2.4	44.1	5.0	7.7	0.8
Zytel HTN*	64.1 ± 2.3	41.0 ± 1.4	44.1 ± 1.1	39.3	9.7	8.3	2.8
Glass 1	48.0 ± 2.5	38.5 ± 1.5	36.0 ± 0.8	40.4	14.1	21.4	2.3
Glass 2	37.3 ± 1.5	44.0 ± 1.1	30.0 ± 1.4	37.5	19.0	31.0	2.3

* Zytel HTN51G35HSL NC010, 35% glass reinforced, heat stabilised, lubricated high performance polyamide resin.

Table 4 Mechanical test conditions and the respective dimensions of the specimen

Conditions	Test method	Based on	Specimen dimensions
Temperature: 23 ± 2°C	3PB	BS EN ISO 3325	40 mm x 20 mm x 4 mm*
Load cell: 5 KN	Iosipescu	BS EN 12289	76 mm x 20 mm x 4 mm**
Cross-head speed: 1 mm/min	DVN	Double v-notch test (non-standard test)	80 mm x 20 mm x 4 mm**
Compression mode			

* span distance: 22.5mm ** notch angle/depth: 90°/4.5mm

Table 5 Band assignments observed in the FTIR spectra.

Band no.	Wavenumber (cm^{-1})	Functional groups*
Boron carbide		
1	3458	ν_a(O-H)
2	1542	ν(C-B-C)
3	1435-1404	ν(B-O)
4	1074	ν(B-C)
5	842	free icosahedral B_{12}
6	701	ν(B-OH)
Silane non hydrolysed		
7,8	2942-2840	ν_a(C–H) CH_3 CH_2
9	1466	δ_{sc}(C-H) CH_2
10	1339	ρ or δ(C-H) CH_3
11	1254	ν_s(epoxy ring)
12	1191	ν(CH_2-O-CH_2)
13	1075	ν_a(Si-O-CH_3)
14	909	ν_a (epoxy ring)
15	815	ν_s(Si-OCH_3)
16	777	*w*(C-H), CH_2
Silane condensed gel		
17	3390	ν_a(O–H) SiOH
18,19	2934, 2870	ν(C–H) CH_2
20	1724	ν(C=O) Epoxy oxidation
21	1646	δ_s(Si-OH)
22	1198	ν(CH_2-O-CH_2)
23	1091	ν(Si-OH)
24	1008	ν_a(Si-O-Si)
25	907	ν_a(epoxy ring), ν_a(Si-OH)
Silanised boron carbide		
26	3669	ν_a(O–H) SiOH, free OH
27,28	2981,2889	ν(C–H) CH_2
29	1626	ν(C-B-C), δ(O–H) SiOH
30,31	1473,1462	δ_{sc}(C-H) CH_2 or O-CH_2
32	1392	ν(B-O-Si)
33	1250	ν_s(epoxy ring)
34	1152	ν(Si-OH)
35	1095	ν(B-C), ν_a(Si-O-Si)
36	966	ν(Si-OH)
37	941	ν(B-O-Si)
38	879	ν(B-O-Si)
39	850	free icosahedral B_{12},Si-O-Si

* Symbols and abbreviations: *ν* - stretch; *δ* - bend; *w* – wag; *r* - rock; *t* - twist; *τ* - torsion; *sc* - scissor; *s* – symmetric; *a* – asymmetric.

Table 6 Surface free energy of the silane treated BC using various solution pH and concentrations.

BC surface	Surface free energy (mJ/m^2)				
	Total	γs^{LW}	γs^{AB}	γs^{+}	γs^{-}
Untreated	**52.5**	33.7	18.8	16.5	5.4
Corona	**64.3**	38.6	25.7	44.9	3.7
pH3, 0.5% GPS	**38.2**	34.1	4.1	2.3	1.8
pH3, 1.0% GPS	**43.3**	36.3	7.0	7.0	1.8
pH3, 3.0% GPS	**42.7**	37.9	4.8	2.8	2.1
pH5, 0.5% GPS	**40.3**	35.4	4.9	4.8	1.3
pH5, 1.0% GPS	**40.6**	37.5	3.1	13.2	0.2
pH5, 3.0% GPS	**42.5**	38.6	3.8	2.4	1.5
pH7, 0.5% GPS	**37.0**	33.9	3.1	2.1	1.1
pH7, 1.0% GPS	**36.8**	34.3	2.6	2.1	0.8
pH7, 3.0% GPS	**42.6**	38.0	4.7	3.9	1.4
pH9, 0.5% GPS	**43.7**	37.2	6.5	4.9	2.2
pH9, 1.0% GPS	**40.5**	33.7	6.8	4.9	2.3
pH9, 3.0% GPS	**40.1**	33.7	6.4	8.3	1.2

Table 7 Experimental and theoretical adhesive contact angle on the untreated and treated boron carbide.

Surface	Contact angle (º, degrees)	
	θ_{exp} **(sessile drop)**	θ_T **(Eq. 2)**
Untreated	52 ± 0.8	50
Corona	45 ± 2.9	44
pH3, 3%GPS	46 ± 1.7	46
pH5, 3%GPS	47 ± 1.4	45
pH7, 3%GPS	48 ± 2.5	46
pH9, 3%GPS	52 ± 0.9	53